Int J Environ Res (2017) 11:91–98
DOI 10.1007/s41742-017-0010-x

RESEARCH PAPER

Isotherm, Kinetic and Thermodynamic Studies on the Removal of Methylene Blue Dye from Aqueous Solution Using Saw Palmetto Spent

Pradeep Kumar Papegowda[1] · **Akheel Ahmed Syed**[1,2]

Received: 15 February 2017 / Revised: 9 March 2017 / Accepted: 11 March 2017 / Published online: 21 March 2017

Abstract In the present research work Saw palmetto spent (SPS) was used to remove Methylene blue (MB) from aqueous solution economically. SEM and FTIR Studies were made to understand the Morphological properties of the adsorbent. Various parameters of adsorption such as, initial dye concentration, contact time, pH and temperature were studied. Langmuir, Freundlich and Temkin isotherm models were used to explain the adsorption behaviour. Pseudo-first order, pseudo-second order kinetic models and Intra-particle diffusion model were used to study adsorption kinetics. The maximum adsorption capacity value ($q_m = 90.9$ mg g^{-1}) for Langmuir isotherm was near to the experimental value ($q_m = 71.00$ mg g^{-1}). Thermodynamics of adsorption was studied and the values obtained indicate that the process is endothermic and spontaneous. It is confirmed that, SPS is an efficient adsorbent for removal of MB from aqueous solution.

Keywords Saw palmetto spent · Methylene blue · Biosorbent · Adsorption isotherms · Intra-particle diffusion

Introduction

Water pollution is a global issue of great concern. Natural water bodies have continuously been polluted by human activities. Effluents from industries are one of the major water pollutants. Release of dye containing waste into water bodies affects both human and other living system of water bodies (Ambrosio et al. 2012). These industries include textiles, leather, plastic and paper. Removal of dye content from polluted water has become major part of water pollution research as most of these dyes are toxic (Gupta and Suhas 2009). Many research papers have been published on remediation of waste water containing dyes.

Various methods have been developed for the removal of dye from water, for example, photo degradation (Bansal et al. 2009) adsorption (Natali et al. 2011), coagulation, electro coagulation (Nandi and Patel 2013), electro dialysis (Amare et al. 2006), chemical oxidation (Baek et al. 2010a) and microbial degradation (Yang et al. 2016). All these methods have their own advantages and disadvantages, among which adsorption is a simple, rapid and effective method for this purpose. Many researchers have reported the use of different adsorbents for the removal of hazardous dyes from waste water, which includes, degreased coffee bean (Baek et al. 2010b), rice husk (Chowdhury et al. 2011), banana peel (Khalfaoui et al. 2012), root of water hyacinth (Wanyonyi et al. 2014), wood apple shell (Sartape et al. 2013), maize husk leaf (Jalil et al. 2012), potato plant waste (Gupta et al. 2016) and almond shell (Ozdes et al. 2010).

Methylene blue is a cationic dye having heterocyclic aromatic structure (Fig. 1). It is widely used in textile and paper industries. It can cause adverse health effects in humans, such as increased heart beat, cyanosis, jaundice, shock, tissue necrosis and vomiting (Sadhukhan et al. 2016). Hence, it is imperative to remove this dye from polluted water. In the present research work, we have used Saw palmetto spent as an efficient biosorbent for the removal of Methylene blue from aqueous solution.

✉ Pradeep Kumar Papegowda
pradeeppumadi@gmail.com

[1] Department of Studies in Chemistry, University of Mysore, Manasa Gangotri, Mysuru 570006, India

[2] University of Malaya, Kuala Lumpur, Malaysia

Materials and methods

Adsorbate

Methylene blue used in this work was supplied by Loba-Chemie, Mumbai, India. Stock solution of 1000 ppm dye solution was prepared in double distilled water and test solutions of required concentration were prepared by diluting stock solution.

Adsorbent

Saw palmetto spent used in this work was supplied by nutraceutical industries (India). Industrially processed spent material was washed thoroughly with distilled water to remove chemical and physical impurities. The spent was ground to fine powder and again washed with distilled water and dried in sunlight. Dried spent powder is passed through sieves of different pore size and finally dried in hot air oven at 60 °C for 48 h and stored in air tight containers.

Characterization of Adsorbent

The scanning electron micrograph (SEM) of SPS was viewed under scanning electron microscope (Hitachi S3400N, Japan). FTIR (PerkinElmer-Spectrum two, USA) absorption spectra were obtained over the range 4000–600 cm^{-1}.

Adsorption Studies

Batch adsorption experiments were carried out in 250 mL conical flask in an orbital shaker at 160 rpm. All experiments were conducted in triplicate and mean values are reported. The effect of initial dye concentration was carried out by varying the initial MB concentration from 10 to 100 mg L^{-1} using 0.05 g of adsorbent. Kinetic studies were carried out at three different initial dye concentrations 25, 50 and 100 mg L^{-1} using 0.05 g dose of spent. Batch adsorption experiments were carried out over a pH range of 4–11, to study the effect of pH on dye adsorption efficiency of SPS. The solution pH was measured by pH meter (Systronics 802). The pH of dye solution was adjusted using dilute HCl and NaOH. After the adsorption process, pH of the dye solution was adjusted back to pH 7 and measured using double beam UV–Vis spectrophotometer (Systronics 166) at the maximum absorption wavelength of MB ($\lambda_{max} = 618$ nm). The adsorbed amount of MB at equilibrium q_m (mg g^{-1}) was calculated.

$$q_m = (C_0 - C_e)V/W \quad (1)$$

where q_m (mg g^{-1}) is the equilibrium adsorption capacity, C_0 and C_e are the initial and equilibrium concentrations (mg L^{-1}) of MB dye solution, V is the volume (L) and W is the weight (g) of adsorbent.

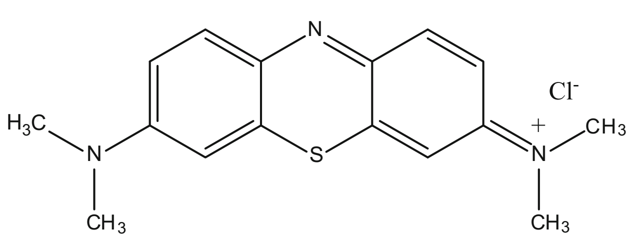

Fig. 1 Structure of Methylene blue

Results and Discussion

Scanning Electron Microscopy (SEM)

The SEM images of SPS, before and after adsorption are shown in Figs. 2 and 3, respectively. Complexity in the morphology of SPS could be seen with porous structure.

After adsorption, there was appreciable change in the morphology of adsorbent which was marked by smoothness of surface due to adsorption of dye molecules, which fits into pores.

Fourier Transform Infrared Spectroscopy (FTIR)

FTIR spectra of SPS in the range of 600–4000 cm^{-1} (Fig. 4) have two main regions of absorption. The bands observed in the range of 1500–1600 cm^{-1} are due to the vibrations of aromatic rings present in the structure of lignin (Salazar-Rabago et al. 2016). A band at 3283 cm^{-1} is associated with stretching of hydroxyl groups of cellulose, hemicelluloses and lignin. A prominent absorption around 2925 cm^{-1} C–H stretching. Absorption band

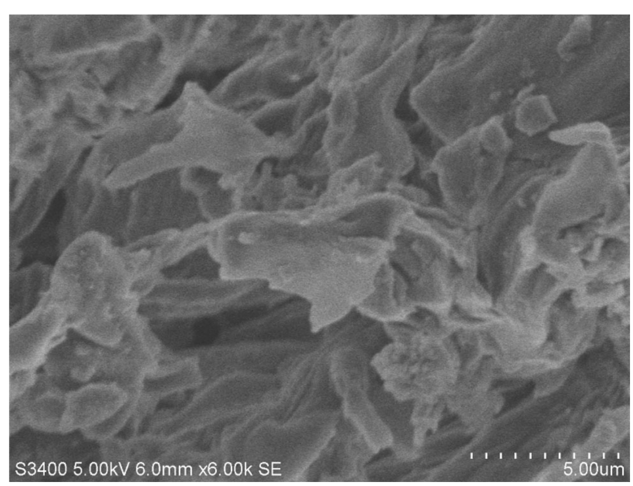

Fig. 2 SEM image of SPS before adsorption

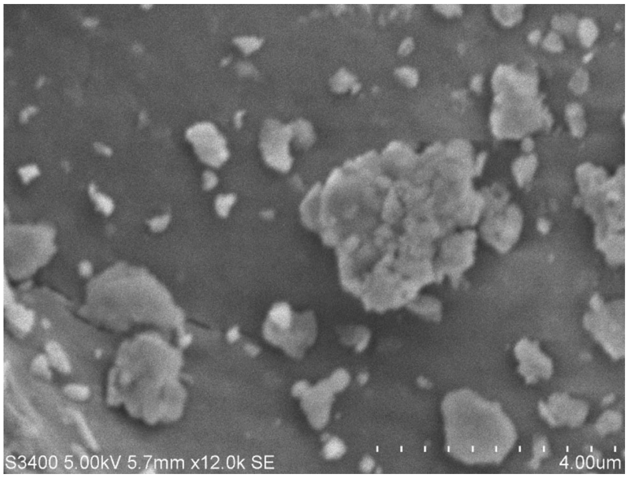

Fig. 3 SEM image of SPS after adsorption

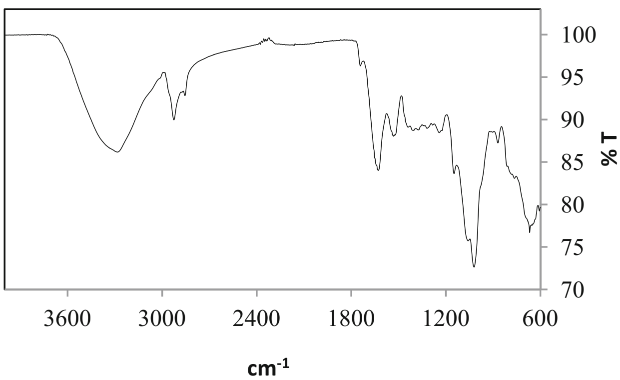

Fig. 4 IR Spectra of SPS

around 1628 cm^{-1} is due to carbonyl group stretching (Gupta et al. 2016). The bands of C–OH stretching were found at 1021 cm^{-1} (Hassan et al. 2013).

Effect of Initial Dye Concentration

The effect of initial concentration of MB on adsorption was studied over a range of 10–120 mg L^{-1}. q_m increased from 8 to 70 mg g^{-1} with the increase in MB concentration from 10 to 90 mg L^{-1}. This may be due to increase in the driving force of the concentration gradient with the increase in the initial MB concentration (Hameed et al. 2008). When initial MB concentration was increased above 90 mg $L^{-1,}$ there was no significant change in the q_m. This may be due to saturation of the adsorbent for further uptake of dye (Fig. 5).

Effect of pH

The pH is an important factor that affects adsorption, because surface charge of adsorbent is decided by pH of

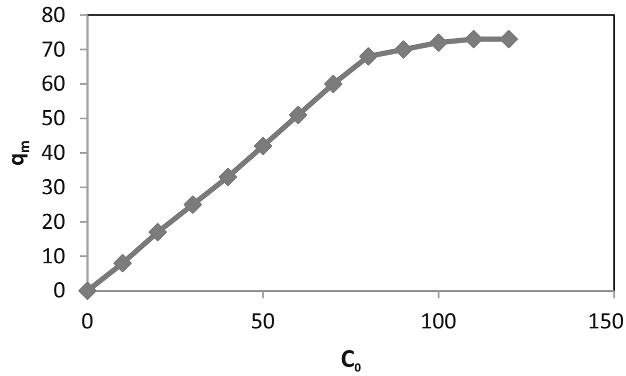

Fig. 5 Effect of initial dye concentration on q_m

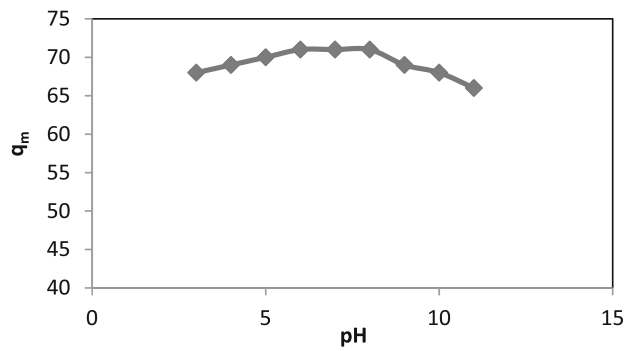

Fig. 6 Effect of pH on q_m

the solution. Adsorption experiments were performed to study the effect of pH with initial dye concentration of 90 mg L^{-1}. From Fig. 6, it can be seen that q_m increases from 68 to 71 mg g^{-1} when the pH was changed from 3 to 6, q_m remains same in the pH range of 6–8, further increase in pH above 8, the q_m gradually decreases and reaches 66 mg g^{-1} at pH 11. The solution pH not only changes the binding sites of the adsorbent but also affects aqueous chemistry. At lower pH the binding sites of adsorbent would be surrounded by H^+ ions which competes with MB, hence q_m decreases at lower pH (Khalfaoui et al. 2012). As the pH increases towards neutral, q_m increases gradually reaches maximum at pH 6. When the pH was increased above 8, there was a slight depression in q_m.

Adsorption Isotherm

Isotherm studies are very important for better understanding of adsorption process. In the present research work commonly used Langmuir, Freundlich and Temkin isotherms were used to explain adsorbate–adsorbent interaction. Langmuir isotherm assumes monolayer adsorption on uniform surface containing limited numbers of sites (Gupta et al. 2016).

Table 1 Adsorption Isotherm constants and correlation coefficients

q_m	Langmuir isotherm			Freundlich isotherm			Temkin isotherm		
	b	R_L	R^2	K_F	n	R^2	A	B	R^2
90.909	0.110	0.0833	0.959	3.033	1.945	0.786	0.989	48.72	0.835

The linear form of Langmuir isotherm is given by the following equation;

$$C_e/q_m = (1/bq_m) + (1/q_m)\,C_e \tag{2}$$

where, q_m is the amount of dye adsorbed per unit mass of adsorbent (mg g^{-1}), C_e is the equilibrium concentration of the adsorbate in solution (mg L^{-1}), Langmuir constant q_m is the monolayer sorption capacity and constant b is related to adsorption energy (L mg^{-1}). q_m and b can be calculated from the slope and intercept of the linear plot of C_e/q_m versus C_e.

Freundlich isotherm model is an empirical equation that describes adsorption process based on a heterogeneous surface. Linear form of the Freundlich expression is presented below:

$$\log q_m = \log K_f + n_f \log C_e \tag{3}$$

The Freundlich constants K_f and n_f are calculated from the plots of log q_m versus log C_e. K_f is related to adsorption capacity and n_f is the measure of adsorption intensity or surface heterogeneity. The value of n_f ranges between 0 and 1, the adsorption becomes more heterogeneous as its value gets closer to zero (Akar et al. 2013).

Temkin describes the process by considering some indirect adsorbate–adsorbate interactions on adsorption (Khalfaoui et al. 2012). This isotherm explains that the linear decrease in heat of adsorption of all the molecules in the layer is the impact of these interactions. The linear form of Temkin isotherm is:

$$q_m = \frac{RT}{b}\ln A + \frac{RT}{b}\ln C_e \quad \text{with} B = \frac{\mathrm{RT}}{\mathrm{b}}, \tag{4}$$

where, q_m is adsorption capacity (mg g^{-1}), C_e is equilibrium dye concentration (mg L^{-1}). A and B are Temkin constants, related to equilibrium binding constant (L g^{-1}) and heat of adsorption (J mol^{-1}) respectively. The values of A and B can be calculated from intercept and slope of the linear plot q_m versus lnC_e. The values of constants and correlation coefficients of all the three isotherm models are presented in Table 1.

The data obtained experimentally found to fit best with Langmuir isotherm model with regression coefficient (R^2) 0.959, which indicates the monolayer adsorption of MB onto SPS. The value of R_L (0.0833) also supports the feasibility of this isotherm, which describes the shape of isotherm to be either favourable ($0 < R_L < 1$), unfavourable ($R_L > 1$) or irreversible ($R_L = 0$) (Sartape et al. 2013) (Figs. 7, 8, 9).

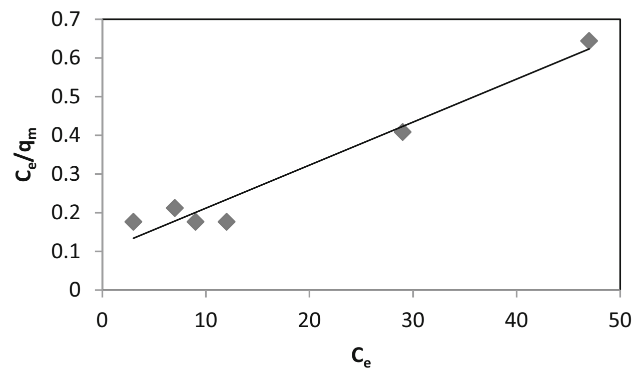

Fig. 7 Langmuir adsorption isotherm

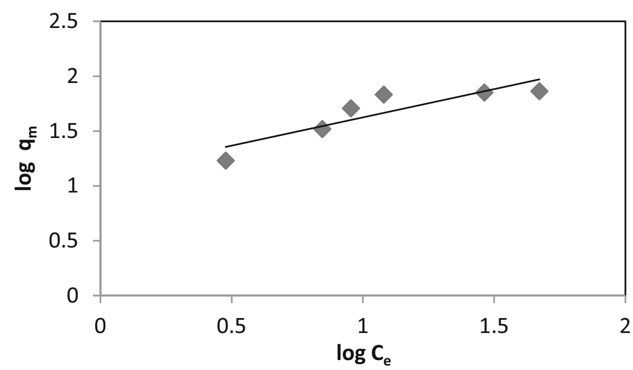

Fig. 8 Freundlich adsorption isotherm

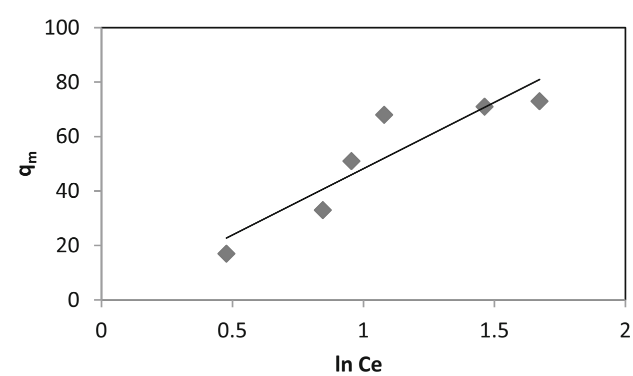

Fig. 9 Temkin adsorption isotherm

Kinetic Studies

Study of kinetics is an important part of adsorption research as it explains the rate of adsorption from which mechanism of the process and rate controlling steps could be predicted.

In the present study, we used three different models to predict the adsorption kinetics of MB onto SPS (Pseudo-first order, Pseudo-second order and Intra-particle diffusion model).

Pseudo-First Order Kinetic Model

The differential rate equation is

$$dq_t/dt = k_1(q_m - q_t) \quad (5)$$

where, k_1 is the pseudo-first order rate constant (min^{-1}), q_t and q_m are the amount of dye adsorbed at any time t (mg g^{-1}) and at equilibrium (mg g^{-1}), respectively. Integrating Eq. (5) using the boundary condition, $q_t = 0$ at $t = 0$ leads to:

$$\log(q_m - q_t) = \log q_m - (k_1/2.303)t \quad (6)$$

The values of k_1 and q_m were calculated from the slope and intercept of the linear plots of log ($q_m - q_t$) versus t (Fig. 10) respectively, and presented in Table 2.

Pseudo-Second Order Kinetic Model

The pseudo-second order kinetic model can be presented as:

$$dq_t/dt = k_2(q_m - q_t)^2 \quad (7)$$

where, k_2 is the pseudo-second order rate constant (g mg^{-1} min^{-1}), q_t and q_m are the amount of dye adsorbed at any time t (mg g^{-1}) and at equilibrium (mg g^{-1}), respectively. Integrating Eq. (7) using the boundary condition, $q_t = 0$ at $t = 0$ leads to:

$$t/q_t = 1/k_2q_m^2 + t/q_m \quad (8)$$

The values of k_2 and q_m were calculated from intercept and slope of the linear plots of t/q_t versus t (Fig. 11), respectively, and presented in Table 2.

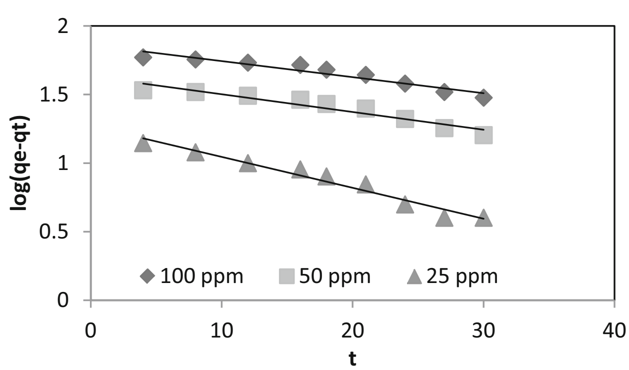

Fig. 10 Pseudo-first order kinetic model

Intra-Particle Diffusion Model

This model was developed by Weber and Morriss (1963), which can be expressed as:

$$q_t = K_i t^{1/2} + C \quad (9)$$

where, K_i is intra-particle diffusion rate constant (mg g^{-1} $min^{1/2}$) and C is the measure of boundary layer effect. Values of K_i and C were obtained from slope and intercept of the plots of q_t versus $t^{1/2}$. According to this model, the plots of q_t versus $t^{1/2}$ should be linear if intraparticle diffusion is involved in the adsorption process and diffusion is rate controlling step if the line passes through origin (Chen et al. 2003) (Fig. 12).

The parameter of all the models used to study the kinetics of the adsorption models are summarized in the Table 2. The plot of intraparticle diffusion model did not pass through origin, which indicates, intraparticle diffusion is not only the rate limiting step, and some other factors may also control the rate of adsorption, which may be operating simultaneously (Yakout and Elsherif 2010). The correlation coefficients R^2, for the pseudo-first-order model (R^2 0.987–0.996) were greater than that of the intraparticle diffusion coefficients (R^2 0.882–0.981), which suggest chemisorption mechanism (Ho and McKay 1998).

Effect of Temperature

The adsorption studies were carried out at 303, 313, 323 and 333 K and the results are shown in Fig. 13. It was observed that as the temperature increased the adsorption capacity also increased, which indicates that the process is endothermic in nature. Change in temperature of the system may alter the porosity of the biosorbent due to

Table 2 Kinetic parameters

Initial dye concentration (mg L^{-1})	q_m exp	Pseudo-first order			Pseudo-second order			Intra-particle diffusion model	
		q_m cal	k_1	R^2	q_m cal	K_2	R^2	K_i	R^2
25	21	23	0.108	0.996	34	0.0023	0.943	3.05	0.981
50	42	39	0.119	0.983	62	0.0015	0.960	5.38	0.891
100	71	76	0.103	0.987	125	0.0006	0.952	8.66	0.882

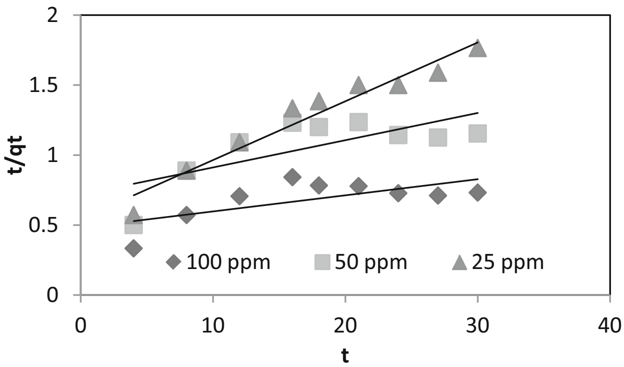

Fig. 11 Pseudo-second order kinetic model

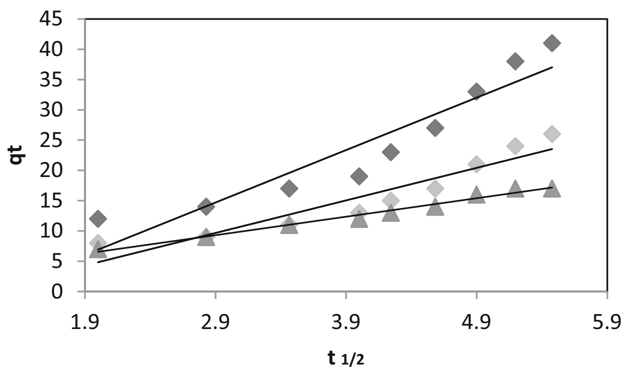

Fig. 12 Intra-particle diffusion model

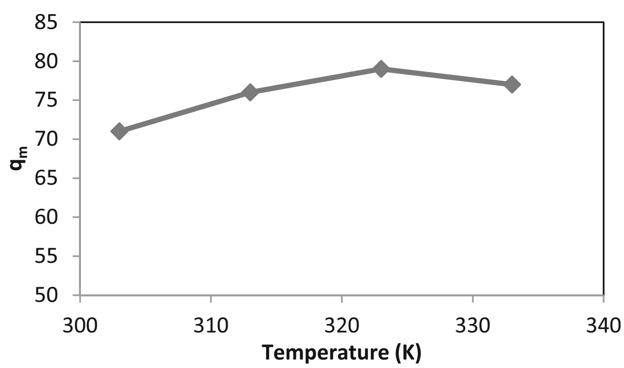

Fig. 13 Effect of temperature on q_m

swelling, which may influence the intraparticle movement of dye molecules (Singh and Srivastava 1999; Aksu et al. 2008).

Thermodynamics of Adsorption

The important factors that are to be considered in the adsorption process are energy and entropy. The standard

Table 3 Thermodynamic parameters

ΔH^0 (kJ mol^{-1})	ΔS^0 (kJ mol^{-1})	ΔG^0 (kJ mol^{-1})			
		303 K	313 K	323 K	333 K
70.96	0.34	−31.18	−37.13	−41.91	−40.68

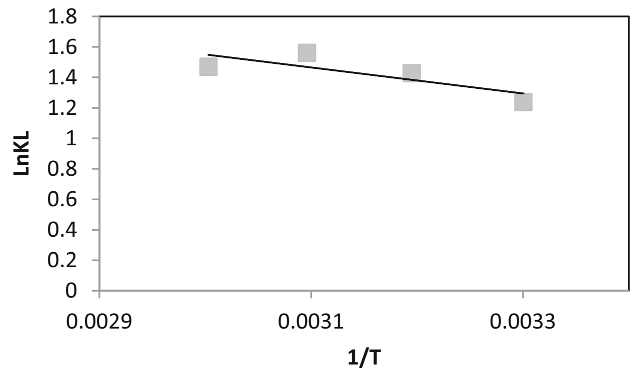

Fig. 14 van't Hoff plot for the adsorption of MB onto SPS

Gibbs free energy change ($\Delta G°$) is the measure of spontaneity of the adsorption process. Significant adsorption occurs, when the $\Delta G°$ of adsorption becomes negative, and these thermodynamic parameters were calculated using van't Hoff and Gibbs–Helmholtz equations.

$$K_L = \frac{C_0}{C_e} \quad (10)$$

$$\Delta G° = -RT \ln K_L \quad (11)$$

$$\ln K_L = {}^{\Delta S°}/_{R} - {}^{\Delta H°}/_{RT} \quad (12)$$

where, C_0 and C_e are the initial and equilibrium concentration (mg L^{-1}) of dye in solution, T is the temperature (K) and K_L is the Langmuir equilibrium constant (L mol^{-1}). The value of ΔG^0 was calculated from Eq. (11), the slope and intercept of the van't Hoff plots of ln(K_L) versus 1/T were used to determine the values of ΔH^0 and ΔS^0 (Table 3; Fig. 14).

Positive value of ΔH^0 (70.96 kJ mol^{-1}) indicates that, the adsorption process is endothermic, and the possibility of physical adsorption (Hema and Arivoli 2008). Negative values of ΔG^0 indicates that adsorption of MB onto SPS is favourable and spontaneous. Adsorption process was more spontaneous at higher temperature as the ΔG^0 values decreased from −31.18 to −41.91 kJ mol^{-1} with increasing temperature (Chu et al. 2004). Increase in randomness at the solid–solution interface was indicated by the positive value of ΔS^0 (0.34 kJ mol^{-1}) (Namasivayam and Kavitha 2002).

Conclusion

In the present study, SPS has been successfully used as an economical and eco-friendly adsorbent for the remediation of a toxic dye, Methylene Blue from its aqueous solution. Maximum adsorption capacity was $q_m = 71.00$ mg g^{-1}, and it is near to the value obtained by Langmuir ($q_m = 90.9$ mg g^{-1}) with correlation coefficient (R^2) of 0.959. The kinetic data obtained experimentally, better fits with pseudo-first order kinetic model. Possible mechanisms of MB–SPS interactions that can occur in system have been discussed. From thermodynamic parameters it is clear that the adsorption process is endothermic and spontaneous. Finally it could be concluded that, SPS can be used as a fast and effective biosorbent for the removal of MB from aqueous solutions.

Acknowledgements The authors gratefully acknowledge University Grants Commission, Government of India for the award of Research Fellowship in Science for meritorious students (Pradeep Kumar P).

References

Akar E, Altinisik A, Seki Y (2013) Using of activated carbon produced from spent tea leaves for the removal of malachite green from aqueous solution. Ecol Eng 52:19–27. doi:10.1016/j.ecoleng.2012.12.032

Aksu Z, Tatlı AI, Ozlem Tunc O (2008) A comparative adsorption/biosorption study of acid blue 161: effect of temperature on equilibrium and kinetic parameters. Chem Eng J 142:23–39. doi:10.1016/j.cej.2007.11.005

Amare B, Chandravanshi BS, Moges G, Megersa N (2006) Hexafluorotantalate(V)-selective coated graphite electrode based on malachite green. Anal Lett 30:457–474. doi:10.1080/00032719708001794

Ambrosio ST, Vilar Junior JC, da Silva CAA, Okada K, Nascimento AE, Longo RL, Campos-Takaki GM (2012) A biosorption isotherm model for the removal of reactive azo dyes by inactivated mycelia of cunninghamella elegans UCP542. Molecules 17:452–462. doi:10.3390/molecules17010452

Baek MH, Ijagbemi CO, Kim DS (2010a) Spectroscopic studies on the oxidative decomposition of Malachite Green using ozone. J Environ Sci Health, Part A 45:630–636. doi:10.1080/10934521003595779

Baek MH, Ijagbemi CO, Se-Jin O, Kim DS (2010b) Removal of malachite green from aqueous solution using degreased coffee bean. J Hazard Mater 176:820–828. doi:10.1016/j.jhazmat.2009.11.110 **(Epub 2009 Nov 27)**

Bansal P, Bhullar N, Sud D (2009) Studies on photodegradation of malachite green using TiO_2/ZnO photocatalyst. Desalin Water Treat 12:108–113. doi:10.5004/dwt.2009.944

Chen JP, Wu S, Chong KH (2003) Surface modification of a granular activated carbon by citric acid for enhancement of copper adsorption. Carbon 41:979–1986. doi:10.1016/S0008-6223(03),00197-0

Chowdhury S, Mishra R, Saha P, Kushwaha P (2011) Adsorption thermodynamics, kinetics and isosteric heat of adsorption of malachite green onto chemically modified rice husk. Desalination 265:159–168. doi:10.1016/j.desal.2010.07.047

Chu BS, Baharin BS, Che Man YB, Quek SY (2004) Separation of vitamin E from palm fatty acid distillate using silica. I. Equilibrium of batch adsorption. J Food Eng 62:97–103. doi:10.1016/S0260-8774(03)00196-1

Gupta VK, Suhas (2009) Application of low-cost adsorbents for dye removal: a review. J Environ Manage 90:2313–2342. doi:10.1016/j.jenvman.2008.11.017

Gupta N, Kushwaha AK, Chattopadhyaya MC (2016) Application of potato (*Solanum tuberosum*) plant wastes for the removal of methylene blue and malachite green dye from aqueous solution. Arabian J Chem 9:S707–S716. doi:10.1016/j.arabjc.2011.07.021

Hameed BH, Mahmoud DK, Ahmad AL (2008) Sorption of basic dye from aqueous solution by pomelo (*Citrus grandis*) peel in a batch system. Colloids Surf A 316:78–84. doi:10.1016/j.colsurfa.2007.08.033

Hassan W, Farooq U, Ahmad M et al (2013) Potential biosorbent, *Haloxylon recurvum* plant stems, for the removal of methylene blue dye. Arabian J Chem. doi:10.1016/j.arabjc.2013.05.002

Hema M, Arivoli S (2008) Adsorption kinetics and thermodynamics of malachite green dye unto acid activated low cost carbon. J Appl Sci Environ Manage 12:43–51

Ho YS, McKay G (1998) Sorption of dye from aqueous solution by peat. Chem Eng J 70:115–124. doi:10.1016/S0923-0467(98),00076-1

Jalil AA, Triwahyono S, Yaakob MR et al (2012) Utilization of bivalve shell-treated *Zea mays* L. (maize) husk leaf as a low-cost biosorbent for enhanced adsorption of malachite green. Bioresour Technol 120:218–224. doi:10.1016/j.biortech.2012.06.066

Khalfaoui A, Meniai AH, Derbal K (2012) Isotherm and kinetics study of biosorption of cationic dye onto banana peel. Energy Procedia 19:286–295. doi:10.1016/j.egypro.2012.05.208

Namasivayam C, Kavitha D (2002) Removal of Congo Red from water by adsorption onto activated carbon prepared from coir pith, an agricultural solid waste. Dyes Pigm 54:47–58. doi:10.1016/S0143-7208(02)00025-6

Nandi BK, Patel S (2013) Effects of operational parameters on the removal of brilliant green dye from aqueous solutions by electrocoagulation. Arabian J Chem. doi:10.1016/j.arabjc.2013.11.032

Natali FC, Eder CL, Isis SP, Camila VA, Betina R, Rodrigo BP, Wagner SA, Simone FPP (2011) Application of cupuassu shell as biosorbent for the removal of textile dyes from aqueous solution. J Environ Manage 92:1237–1247. doi:10.1016/j.jenvman.2010.12.010

Ozdes D, Gundogdu A, Duran C, Senturk HB (2010) Evaluation of adsorption characteristics of malachite greenonto almond shell (*Prunus dulcis*). Sep Sci Technol 45:2076–2085. doi:10.1080/01496395.2010.504479

Sadhukhan B, Mondal NK, Chattoraj S (2016) Optimisation using central composite design (CCD) and the desirability function for sorption of methylene blue from aqueous solution onto Lemna major. Karbala Int J Mod Sci 2:145–155. doi:10.1016/j.kijoms.2016.03.005

Salazar-Rabago JJ, Leyva-Ramos R, Rivera-Utrilla J et al (2016) Biosorption mechanism of methylene blue from aqueous solution onto white pine (*Pinus durangensis*) sawdust: effect of operating conditions. doi:10.1016/j.serj.2016.11.009

Sartape AS, Mandhare AM, Jadhav VV et al (2013) Removal of malachite green dye from aqueous solution with adsorption technique using *Limonia acidissima* (wood apple) shell as low cost adsorbent. Arabian J Chem. doi:10.1016/j.arabjc.2013.12.019

Singh DK, Srivastava B (1999) Removal of basic dyes from aqueous solutions by chemically treated psidium guyava leaves. Indian J Environ Health 41:333–345

Wanyonyi WC, Onyari JM, Shiundu PM (2014) Adsorption of Congo Red dye from aqueous solutions using roots of eichhornia crassipes: kinetic and equilibrium studies. Energy Procedia 50:862–869. doi:10.1016/j.egypro.2014.06.105

Weber WJ, Morris JC (1963) Kinetics of adsorption carbon from solutions. J Sanit Eng Div ASCE 89:31–60

Yakout SM, Elsherif E (2010) Batch kinetics, isotherm and thermodynamic studies of adsorption of strontium from aqueous solutions onto low cost rice-straw based carbons. Carbon Sci Tech 3:144–153

Yang P, Shi W, Wang H, Liu H (2016) Screening of freshwater fungi for decolorizing multiple synthetic dyes. Braz J Microbiol 47:828–834. doi:10.1016/j.bjm.2016.06.010